International Conference on Applied Energy 2019
Aug 12-15, 2019, Västerås, Sweden
Paper ID: 491

A COMPUTATIONAL FLUID DYNAMICS ANALYSIS OF AN INDIRECT EVAPORATIVE COOLER EMPLOYING THE PARTICLE TRANSPORT METHOD

Torsten Berning*, Henrik Sørensen, Mads Pagh Nielsen

Department of Energy Technology, Aalborg University, Denmark

ABSTRACT

A numerical analysis of heat and mass transfer in an indirect evaporative cooling system for building applications is presented. The model is based on the computational fluid dynamics software CFX-4 and makes use of the built-in Spray Drier model to study the droplet movement, heat transfer, and evaporation rate from the water to the exhaust air. The effect of the average droplet size and mass flow rate as well as the angle of the heat exchanger on the cooling performance to the supply air is reported.

Keywords: energy conservation in buildings

NOMENCLATURE

Abbreviations	
CFD	Computational fluid dynamics
IEC	Indirect evaporative cooling
Nu	Nusselt number
Re	Reynolds number
Sh	Sherwood number
Symbols	
$\mathbf{B}$	Body force vector [N/m^3]
$\mathbf{C}$	Computational particle velocity [m]
C_D	Drag factor [-]
c_p	Specific heat [J/kg]
D	Diffusivity [m^2/s]
d_h	Hydraulic channel diameter [m]
d	Particle diameter [m]
F	Force on particle [N]
$\mathbf{g}$	Gravity vector [9.81 kg-m/s^2]
H	Total specific enthalpy [J/kg]
h	Static specific enthalpy [J/kg]
p	Pressure [Pa]
P_{vap}	Vaporization pressure [Pa]
$\dot{m}$	Mass flux [kg/s]
Q_c	Convective particle heat transfer [W]
Q	Cooling power [W]
R	Gas constant [8.314 J/mole-K]
R_C	Resistance constant [N-s/m^2]
R_F	Resistance speed factor [N-s^2/m]
T	Temperature [K]
t	Time [s]
$\mathbf{U}$	Velocity vector [m/s]
$\mathbf{u}$	Physical particle velocity [m/s]
V	Heat of vaporization [J/kg]
$\mathbf{v_R}$	Relative particle velocity [m/s]
W	Molecular weight [kg/mole]
X_i	Molar fraction of species i [-]
$\mathbf{x}$	Position variable [m]
Y_i	Mass fraction of species i [-]
α	Tilt angle [°]
β	Resistance speed constant [-]
λ	Thermal conductivity [W/m-K]
ρ	Density [kg/m^3]
μ	Dynamic viscosity [kg/m-s]
ξ	Particle position [m]

1. INTRODUCTION

Indirect evaporative cooling (IEC) is a simple and well-established method to effectively cool down incoming air via heat transfer to exhaust air where liquid water is added to induce evaporative cooling. The main drawback of this method is the water usage [1]. Moreover, the performance of these devices can be limited by the heat transfer lay-out [2]. Because the heat and mass transfer in IECs is quite complex, numerical models have recently been developed to gain a better

Selection and peer-review under responsibility of the scientific committee of the 11th Int. Conf. on Applied Energy (ICAE2019).

fundamental understanding. So far, the majority of modelling studies have employed a two-dimensional. finite element approach (e.g. [2, 3]), despite the fact that the methods of computational fluid dynamics are very well suited for this type of question. Jafarian et al. [1] were among the few who employed the CFD modelling tool Open FOAM to develop a 3—dimensional model of a regenerative IEC and modified the boundary condition on the wet side. In most studies, however, the source of the water was not treated, but it was assumed to exist in form of a thin layer on the wet channel surface.

It is the goal of the current analysis to shed light into the physics occurring during an evaporative cooling process. In particular, the effect of the mass flow rate and the droplet size of the injected water as well as the tilting angle of the IEC was investigated using computational fluid dynamics (CFD) combined with a particle transport model.

2. MODEL DESCRIPTION

The CFD model is based on the commercial software package CFX-4 (ANSYS Inc.), and the implemented Spray Drier model was employed to track the flow of water droplets and the evaporation rate at exhaust side of the heat exchanger. The details of the model will be described below.

2.1 Model geometry and computational grid

The geometry is three-dimensional and consists of a plate heat exchanger where the primary and secondary air streams are separated by an aluminium sheet. The flow arrangement is counter-flow and the water is sprayed into the secondary air. The primary air stream is also called the product or supply air stream while the secondary air stream is often referred to as the working or exhaust air stream.

The entire geometry as shown in Fig 1 is sub-divided into 9 computational Blocks. Blocks 1-3 represent the primary air region, Blocks 4-6 represent the aluminium sheet which has been defined as a heat conducting solid, and Blocks 7-9 represent the secondary air region.

The actual physical design has corrugated flow channels on both sides to guide the air and to keep the distances between any two channels. Depending on the required total air flow there can be several hundred of these single plates. In our simplified model, the plates are considered to be flat.

In order to account for the corrugated channels, the computational blocks in the center of both air streams (Blocks 2 and 8) are designated as porous media with a resistance term to match the Hagen-Poisseuille equation in the channel direction (*x*-direction) and with a resistance that is two orders of magnitude higher in the lateral direction (*y*-direction) to prevent cross flow. The droplets that are added to the secondary air stream interact with the flow, but in general are not prevented from crossing channels in the *y*-direction, driven by gravity.

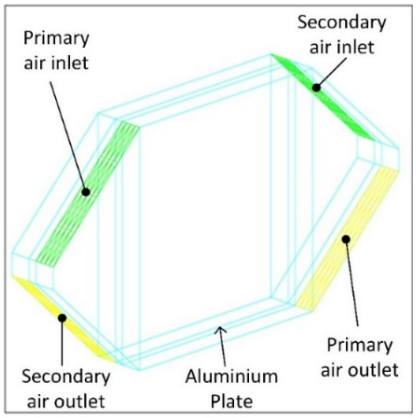

Fig 1: Computational domain.

The overall dimensions are a total length of 45 cm and a height of 30 cm. Owing to symmetry, only half of the channel height is modeled. Thus, the channel height is 2.5 mm and the thickness of the aluminum sheet is 0.5 mm. The computational mesh is an IJK-block structured mesh with hexahedral cells, and it is shown in Fig 2. The total number of cells is 53,000. A grid refinement study has shown that this grid is the best compromise between computational speed and modelling accuracy.

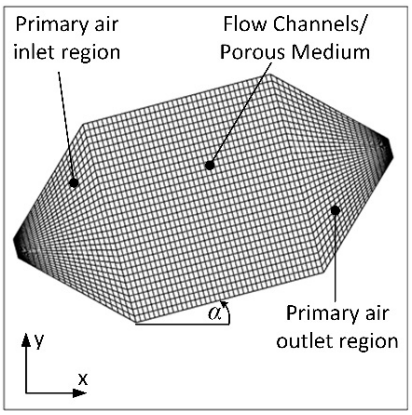

Fig 2: Computational grid and direction conventions.

2.2 Model equations

For the gas phase, the laminar three-dimensional, steady-state Navier-Stokes equations are solved at both sides of the heat exchanger. In addition, one mass fraction equation for the water vapor is solved for.

The detailed conservation equations are [4]:

Mass: $$\nabla \bullet \left(\rho \mathbf{U} \right) = 0$$

Momentum: $$\nabla \bullet \left(\rho \mathbf{U} \otimes \mathbf{U} \right) - \mu \left(\nabla \mathbf{U} + \left(\nabla \mathbf{U} \right)^T \right) = \mathbf{B} + \nabla \bullet \left(-p\delta + \left(\varsigma - 2/3\,\mu \right) \nabla \bullet \mathbf{U}\delta \right)$$

Energy: $$\nabla \bullet \left(\rho \mathbf{U} H \right) - \nabla \bullet \left(\lambda \nabla T \right) = 0$$

In the momentum equations, $\mathbf{B}$ is the body force [4]:

$$\mathbf{B} = \mathbf{B_F} - \left(\mathbf{R_C} + \mathbf{R_F} \left| \mathbf{v} \right|^{\beta} \right) \mathbf{v}$$

In order to model the Hagen-Poisseuille equation in the channels of the heat exchanger (Blocks 2 and 8), $\mathbf{B_F}$ and $\mathbf{R_F}$ were set to zero and only the resistance constant $\mathbf{R_C}$ was specified:

$$\mathbf{R_C} = 32\,\mu / d_h^2$$

Here, d_h is the hydraulic diameter of the channels (4.24 mm). The porosity in the channel regions is set to 0.5, and this leads to an acceleration of the fluxes in the channel region compared to the inlet region.

In the energy equation, H is the total enthalpy that depends on the static (thermodynamic) enthalpy *h(T, p)* according to [4]:

$$H = h + 1/2\,\mathbf{U}^2$$

The thermal conductivity is denoted λ. In the solid region the energy equation simplifies to:

$$\nabla \bullet \left(\lambda_s \nabla T \right) = 0$$

The system of equations is closed by the ideal gas law:

$$\rho = pW / RT$$

Where W is the molecular weight of air (28.84 kg/kmol) and R is the universal gas constant.

The conservation equation for water vapor in the gas phase is [4]:

$$\nabla \bullet \left(\rho \mathbf{U} Y_{H_2O} \right) - \nabla \bullet \left(\rho D \nabla Y_{H_2O} \right) = 0$$

Where Y_{H2O} is the mass fraction of water vapor and D is the binary diffusion coefficient of water vapor in air (2.16×10^{-6} m^2/s).

For the particle transport model in the Lagrangian reference frame, the partial differential equation is solved. This equation for the position of a particle is given as [4]:

$$d\boldsymbol{\xi} / dt = \mathbf{C}$$

Where $\boldsymbol{\xi}$ is the computational position, t is time and $\mathbf{C}$ is computational velocity. The latter is obtained from the physical velocity of the particles $\mathbf{u}$ according to [4]:

$$\mathbf{C} = \left(d\mathbf{x} / d\xi \right)^{-1} \mathbf{u}$$

The momentum equations for the disperse phase result directly from Newton's second law [4]:

$$m \left(d\mathbf{u} / dt \right) = \mathbf{F}$$

where $\mathbf{F}$ is the force on the particle and m is its mass. The major component of the force term is the drag exerted on the particle by the continuous phase [4]:

$$\mathbf{F}_D = 1/8\,\pi d^2 \rho \mathbf{C_D} \left| v_R \right| v_R$$

where the drag factor is given by [4]:

$$\mathbf{C_D} = 24 / \mathrm{Re} \left(1 + 0.15\,\mathrm{Re}^{0.687} \right)$$

And the particle Reynolds number is defined as [4]:

$$\mathrm{Re} = \left(\rho \left| v_R \right| d \right) / \mu$$

In addition to the drag force, the buoyancy force is accounted for [4]:

$$\mathbf{F}_B = 1/6\,\pi d^3 \left(\rho_P - \rho \right) \mathbf{g}$$

In the CFX-4 Spray Drier model that we employed the particle mass transfer depends on whether the particle is above or below the boiling point which is described by Antoine's equation:

$$P_{vap} = \exp \left(A - B / \left(T + C \right) \right)$$

If the saturation pressure is given in [Pa] and the temperature in [K], then the coefficients for water are A=23.296, B=3816.44 and C=-46.13 [4].

When the particle is above the boiling point, the mass transfer is determined by the convective heat transfer [4]:

$$dm / dt = -Q_C / V$$

where V is the heat of vaporization (2.265×10^6 J/kg). The rate of convective heat transfer is given by [4]:

$$Q_C = \pi d \lambda Nu \left(T_G - T \right)$$

where λ is the thermal conductivity of the fluid, T_G and T are the temperature of the fluid and the particle, and Nu is the Nusselt number given by [4]:

$$Nu = 2 + 0.6\,\mathrm{Re}^{0.5} \left(\mu c_P / \lambda \right)^{1/3}$$

where c_p is the specific heat of the fluid (4186 J/kg).

When the particle is below the boiling point the mass transfer is given by [4]:

$$dm / dt = \pi d D Sh \left(W_C / W_G \right) \log \left(1 - X / 1 - X_G \right)$$

Here, W_C and W_G are the molecular weights of the vapor and the mixture in the continuous phase, while X and X_G are the molar fractions in the drop and in the gas phase. Finally, the Sherwood number Sh is given by [4]:

$$Sh = 2 + 0.6\,\mathrm{Re}^{0.5} \left(\mu / \rho D \right)^{1/3}$$

Where D is the diffusivity.

2.3 Boundary Conditions

The simulations in this study were conducted for similar conditions as prior experiments. The inlet velocities on both sides was 2.44 m/s which corresponds

to the nominal load of the actual design. The inlet relative humidities were 60% on both sides and the inlet temperatures were 26 °C. This resulted in mass flow rates of 1.22×10^{-3} kg/s at both inlets. The amount of water added at the exhaust side in the base case was 10×10^{-6} kg/s. The diameter size distribution was a Rossin Rammler distribution with an prescribed average droplet size and a spread of 3. 200 particles were tracked in 4 different droplet sizes. At both outlets, ambient pressure was applied while zero-gradient conditions were imposed for all other transport equations. Finally, symmetry conditions were applied at the high-z and low-z interfaces.

3. RESULTS

In the current study, the average droplet diameter, the mass flow rate of the water and the tilting angle of the heat exchanger was varied. The parameters are summarized in Table 1.

Table 1: Summary of cases and key parameters.

Case #	$\dot{m}_{water}$ $[g/s]$	$d_{ave,droplet}$ $[microns]$	$Tilt\ \alpha$ [°]	$\dot{m}_{air}$ $[g/s]$
1	0.01	50	0	1.22
2	0.01	50	30	1.22
3	0.01	20	30	1.22
4	0.01	10	30	1.22
5	0.02	10	30	1.22

The most interesting results of the particle transport model are the particle tracks and the local evaporation rate. Figure 3 shows exemplarily the particle tracks and the particle temperature. The streamlines suggest only a weak effect of gravity. In prior experiments, the tilting effect was found to be quite large and the system performance was best at a tilting angle of 30 °.

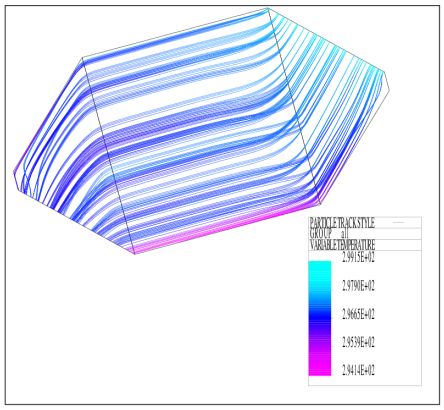

Fig 3: Particle tracks and temperatures.

The calculated temperature distribution on the exhaust side as well as the corresponding distribution on the supply side are exemplarily shown in Fig 4 and Fig 5 for Case #3. In both cases the plane shown is located in the middle of the channel domain. Owing to the random distribution of the particles, the temperature distribution is fairly uneven, but this has no impact on the calculated temperature distribution at the supply side and the calculated cooling power.

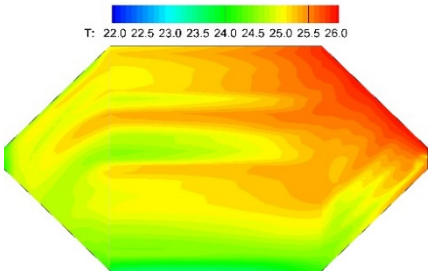

Fig 4: Temperature distribution at the exhaust side.

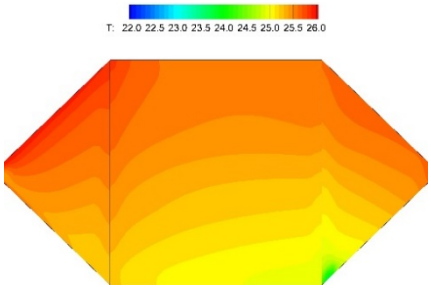

Fig 5: Temperature distribution at the supply side.

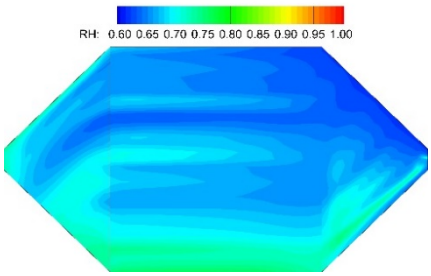

Fig 6: Relative humidity distribution at the exhaust side.

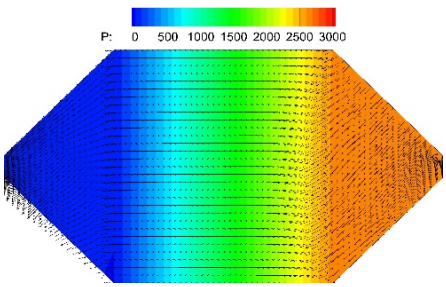

Fig 7: Pressure distribution at the exhaust side.

The relative humidity remains below 100%, shown in Fig 6. Because liquid water is predicted to leave the heat exchanger there is no equilibrium between the gas and the liquid phase. The calculated pressure drop on the exhaust side is shown in Fig 7, and it is predicted to be almost an order of magnitude higher than on the supply side (not shown) which is in the single phase. This pressure drop will depend on the particle size and evaporation rate.

4. DISCUSSION

The main result of interest is the cooling power of the primary air stream (supply air), defined as:

$$Q = \dot{m} c_p \Delta T$$

In addition, the wet-bulb efficiency is used:

$$\eta = \left(T_{db,out} - T_{db,supply}\right) \Big/ \left(T_{db,out} - T_{wb,extract}\right)$$

In the current case, the outside dry bulb temperature is 26 ^{o}C and the wet bulb temperature of the extract air is 20.28 ^{o}C. Hence, if the supply air is cooled down by 2 ^{o}C the wet-bulb efficiency is around 35%.

Table 2 summarizes the key results of the cases investigated. There is a large variation in the efficiency. Overall, the finest droplets lead to the best efficiency. Considering the fact that the inlet temperature of the supply air was 26 °C, a cooling down to 24.25 °C appears to be not satisfactory. Note, however, that these conditions where the outside air is at 26 °C and the exhaust air from the room enters the heat exchanger at 26 °C and at a relative humidity of 60% are quite challenging. While the lowest local temperature on the exhaust side is in the range of 20 °C, depending on the case, this low temperature is unfortunately not transmitted to the supply side which means that the heat exchanger may still be optimized.

In summary, it was found that both the droplet size and the amount of water sprayed into the system had a strong effect on the performance while effect of the titling angle was found to be minor. Clearly, there is still room for further improvement in the current design whose largest advantage is the simplicity.

Table 2: Summary of key results

Case #	$\dot{Q}$ [W]	$T_{db,supply}$	η[%]
1	0.19	25.85	2.7
2	0.19	25.85	2.7
3	0.76	25.38	10.83
4	1.89	24.36	26.86
5	2.14	24.25	30.56

5. CONCLUSIONS

A CFD analysis of an indirect evaporative cooler employing the particle transport method to simulate the interaction of the liquid water droplets with the background air stream has been carried out. It was found that owing to the smaller residence time of the droplets in the heat exchanger, almost none of the droplets evaporated, and the calculated amount of heat transfer from the droplets is far from the theoretical maximum. Only when the average droplet size was decreased to 10 microns a sizeable number of particles actually evaporate completely. The predicted performance of the heat exchanger depends strongly on the droplet size and amount of water sprayed into the system. In general, the CFD model can be employed to identify critical parameters in order to improve the design.

ACKNOWLEDGEMENT

The work was funded by ElForsk, Project Number 350-007.

REFERENCE

[1] Jafarian H., Sayyaadi H., Torabi F. ”A numerical model for a dew-point counter-flow indirect evaporative cooler using a modified boundary condition and considering effects of entrance regions”. Int. J. Refrigeration 2017; 84, 36-51.

[2] Min Y., Chen Y., Yang H., ”Numerical study on indirect evaporative coolers considering condensation: A torouygh comparison between cross and counter flow”, Int. J. Heat and Mass Transfer 2019, 131, 472-486.

[3] De Antonellis S., Joppolo C. M., Liberati P., Milani S. “Modeling and experimental study of an indirect evaporative cooler”, Energy and Buildings 2017, 142, 147-157.

[4] CFX-4 Solver Manual, AEA Technology, 2004.